Chemical Engineering Journal 249 (2014) 293–301

Contents lists available at ScienceDirect

Chemical Engineering Journal

journal homepage: www.elsevier.com/locate/cej

Removing oil droplets from water using a copper-based metal organic frameworks

Kun-Yi Andrew Lin [a,*], Hongta Yang [b], Camille Petit [c], Fu-Kong Hsu [a]

[a] Department of Environmental Engineering, National Chung Hsing University, 250 Kuo-Kuang Road, Taichung, Taiwan, ROC
[b] Department of Chemical Engineering, National Chung Hsing University, 250 Kuo-Kuang Road, Taichung, Taiwan, ROC
[c] Department of Chemical Engineering, Imperial College London, South Kensington Campus, Exhibition Road, London SW7 2AZ, UK

HIGHLIGHTS

- Oil removal from water by a copper-based MOFs, HKUST-1, is demonstrated.
- HKUST-1 exhibits a promising oil-removal capacity of 4000 mg g^{-1}.
- Effects of salts, surfactants, pH of emulsions on removal capacity are examined.
- HKUST-1 can be regenerated conveniently by washing with ethanol.

GRAPHICAL ABSTRACT

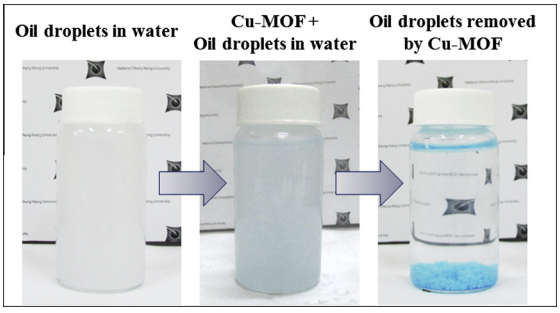

ARTICLE INFO

Article history:
Received 19 February 2014
Received in revised form 24 March 2014
Accepted 26 March 2014
Available online 5 April 2014

Keywords:
Metal–organic frameworks
Oil/water separation
HKUST-1

ABSTRACT

To recover oil during manufacturing processes or to eliminate oil pollution in wastewaters, oil droplets must be separated from water. Among the current techniques for oil removal, adsorption appears to be one of the simplest. Metal Organic Frameworks (MOFs) have recently been proposed as adsorbents to remove contaminants from water owing to their high surface area and versatile tunability. Interestingly, only a few studies looked at the use of MOFs to remove oil droplets and several unknowns remain regarding the mechanism and the potential of this approach. Here, we propose to use a copper-based MOFs, HKUST-1, to separate oil droplets from water. HKUST-1 is synthesized and characterized using XRD, FTIR, N_2 sorption analysis and thermogravimetric analysis. The kinetic and equilibrium constants of the oil/water separation are determined; HKUST-1 exhibits a high removal capacity, about six times higher than a commercial activated carbon. This performance can be further improved via addition of salts and surfactants, and change of pH. HKUST-1 is successfully regenerated via an ethanol-washing process and its capacity remains about constant up to 5 cycles. The kinetics of the oil/water separation follows a pseudo second order, while the adsorption isotherm can be fitted using the Langmuir model.

1. Introduction

Oil droplets in water can be found in many industries such as petroleum [1–3], pharmaceuticals [4,5], food processing [6,7] and metal manufacturing [8]. Domestic wastewater also contains high concentration of oil derived from plant, animal, synthetic fat and human wastes [9]. Separation of oil from water can be desired to recover the oil from manufacturing processes or to eliminate oil pollution in water [10–13].

Up to date, many techniques have been employed to separate oil droplets from water including filtration [14–16], chemical destabilization [17], electrocoagulation [18,19], flotation [20–23], or adsorption. Among these techniques, adsorption appears to be

* Corresponding author. Tel.: +886 422854709.
E-mail address: linky@nchu.edu.tw (K.-Y.A. Lin).

http://dx.doi.org/10.1016/j.cej.2014.03.107
1385-8947/

one of the most attractive methods to remove contaminants owing to its simple design and relatively low initial cost [24]. Common adsorbents for oil removal include granular activated carbon, natural fibers, agricultural wastes and minerals [25–28]. Since the physical and chemical properties of adsorbents (e.g., surface areas, pore volumes, and surface functional groups) significantly influence their removal capacity, strategies to tune these materials must be thoughtfully implemented in order to improve the efficiency of separating oil from water [3].

A new type of porous network material named Metal Organic Frameworks (MOFs) has attracted great attention among the scientific community [29–31]. These materials are synthesized by combining metal ions and organic ligands to form a porous crystalline network. With their exceptional physical and chemical properties, MOFs have had a significant impact on disciplines related to gas storage and adsorption [32–34], catalysis [35–37], drug delivery [34,38], and sensing [39].

Recently, a number of studies started to evaluate the feasibility of MOFs to remove contaminants from water such as metal ions [40], dyes [41], and other organic compounds [42], revealing that MOFs can be stable in the aqueous environment and exhibit great capacity to separate the targeted contaminants. As a promising porous material, we expect MOFs to be capable of removing oil droplets from water. If successful, MOFs could be used not only in wastewater treatments but also for the separation of hydrophobic compounds from hydrophilic solvents in a variety of applications, including biological systems, food processing, pharmaceuticals or analytic chemistry. To the best of our knowledge, only a few studies have been conducted to evaluate this potential application of MOFs-related materials [43,44].

Thus, we propose to use MOFs for the separation of oil droplets from water. In this study, a copper-based MOFs, HKUST-1 (or CuBTC), was selected owing to its stability in water [45] as well as extensive applicability in many fields, including catalysis [46–49], analytic chemistry [50,51], separation [52], gas storage [53], sensor [54], etc. In addition, HKUST-1 is relatively straightforward to synthesize as it is made of commercially available ligands and it forms under mild conditions. The material performance was compared to that of a granular activated carbon. We investigated the reaction kinetics by three common kinetics models: the pseudo first order equation, the pseudo second order equation and the intraparticle diffusion. Adsorption isotherms were also modeled by two common isotherm models: Langmuir isotherm and Freundlich isotherm. We examined the effects of additions of NaCl and CTAB, and change of the pH on the removal capacity. The recyclability was also tested using a rapid and convenient method to regenerate HKUST-1 by washing with ethanol.

2. Experimental

2.1. Materials and methods

Copper acetate monohydrate ($Cu(CO_2CH_3)_2{\cdot}H_2O$) was purchased from Scharlab S.L. (Spain); benzene-1,3,5-tricarboxylic acid (H_3BTC) was purchased from Alfa Aesar (England). D.I. Water (D.I.) was prepared to exhibit less than 18 MΩ cm; ethanol was purchased from Merck. Soybean oil was obtained from Fwusow Industry Co.; sodium chloride (NaCl) pellets and cetrimonium bromide (CTAB) were purchased from Sigma–Aldrich. Granular activated carbon was purchased from Merck (average size of 1.5 mm).

2.2. Synthesis of copper-based MOF, HKUST-1

The copper-based MOFs, HKUST-1, was synthesized and activated according to the procedure reported by Münch and Mertens [50]. In a typical synthesis, 0.299 g (1.5 mmol) copper acetate monohydrate was dissolved in 25 ml D.I. water and heated at 100 °C for 1 h. A 25 ml of ethanol solution containing 0.210 g of H_3BTC was prepared and added to the solution of copper acetate monohydrate. The resulting mixture was stirred at 60 °C for 1 h and subsequently at 25 °C for 12 h. The final product was filtered and washed several times with ethanol to obtain the blue powder. To activate HKUST-1, the blue powder was heated at 100 °C at reduced pressure for 24 h.

2.3. Characterization of HKUST-1

The powder X-ray diffraction patterns (PXRD) of HKUST-1 were obtained using an X-ray diffractometer (PANalytical) with copper as an anode material (40 mA, 45 kV). Infrared (IR) spectroscopic analysis of HKUST-1 was conducted using an infrared spectrometer (Jasco 4100). The surface area of HKUST-1 was determined by a nitrogen adsorption and desorption at 77 K using a Micrometrics ASAP 2020 surface area analyzer. To analyze the morphology of as-synthesized HKUST-1, a field emission scanning electron microscopy (FE-SEM) (JEOL JSM-6700F) was used.

2.4. Batch tests for oil droplets removed by HKUST-1

Oil-in-water (O/W) emulsion was prepared according to the procedure reported by Wang et al. [3]. Typically, a mixture of soybean oil (1 ml) and D.I. water (18 ml) was ultrasonicated using an ultrasonicator (Heat Systems Ultrasonics, USA) to obtain a concentrated O/W emulsion. This emulsion was then diluted to a desired concentration by addition of D.I. water. The concentration of oil droplets in water was measured as reported by Zouboulis and Avranas [21] using a turbidimeter (HACH 2000) with a sensitivity of 0.01 NTU. The emulsion turbidity was then converted to the concentration of oil using a standard reference line which was established by measuring the concentrations of oil in a series of standard O/W emulsions with known turbidities using the chemical oxygen demand method (COD). The conversion of the COD concentrations to the concentrations of soybean oil was calculated based on the average formula of soybean oil (i.e., $C_{55}H_{98}O_6$) [55]. The correlation coefficient of the line (R^2) was higher than 0.99 and the standard reference line was examined periodically to ensure its validity over the course of this study.

The removal of oil droplets from water using HKUST-1 was evaluated by a batch-type adsorption test, in which a 20-ml emulsion with a desired concentration was poured in a glass vial and bulk HKUST-1 powder was then added to the vial. The removal reaction was proceeded in a temperature-controlled orbital shaker at 300 rpm.

2.5. Recyclability test of HKUST-1

A recyclability test of HKUST-1 to remove oil droplets was performed using regenerated HKUST-1. To regenerate HKUST-1, the oil-rich HKUST-1 was dissolved in ethanol and the resulting mixture was placed on the orbital shaker at 300 rpm for 2 h at ambient temperature to remove the oil on HKUST-1. The ethanol-washed HKUST-1 was centrifuged to collect HKUST-1 powder which then was placed in a vacuum oven to remove the residual solvent to obtain the regenerated HKUST-1.

2.6. Thermogravimetric analysis of oil-adsorbed HKUST-1

To investigate weight loss of HKUST-1 and the oil-rich HKUST-1 as a function of temperature, the derivative thermogravimetric (DTG) analysis was conducted using a thermogravmetric analyzer (TGA) (ISI, Michigan, USA) with a carrier gas of nitrogen. The

temperature profile of TGA was programmed to ramp from the ambient temperature to 500 °C at a ramping rate of 10 °C min^{-1}.

3. Results and discussion

3.1. Characterization of HKUST-1

The PXRD patterns of the as-synthesized HKUST-1 is shown in Fig. S1 (see ESI†) and can be readily indexed according to reported patterns of HKUST-1 [40,56]: 15.5° (222), 13.2° (440), 16.3° (422), 17.3° (511), 20.0° (660), 25.8° (731), 29.3° (751), 35.0° (773), 38.9° (828), 46.8° (751). SEM image of the as-synthesized HKUST-1 was also shown as an inset in Fig. S1. The as-synthesized HKUST-1 exhibited a porous structure similar to reported morphologies of HKUST-1 prepared by non-hydrothermal methods in mild conditions (i.e., 25–60 °C) [50,57]. The FT-IR spectrum of the as-synthesized HKUST-1 is plotted in Fig. 1(a) (spectrum at the bottom), in which most of absorbance bands are derived from of benzene-1,3,5-tricarboxylate (BTC): 1374 cm^{-1} was assigned to C—O, 1450 cm^{-1}, 1566 cm^{-1} to C=O, 1646 cm^{-1} to aromatic C=C, and 1718 cm^{-1} to COO^- [58,59]. This spectrum of the as-synthesized HKUST-1 could serve as a baseline to compare with the oil-rich HKUST-1 after the oil/water separation tests. The comparison is discussed in a later section. The N_2 sorption–desorption isotherm of the as-synthesized HKUST-1 is shown in Fig. 1(b). At the relatively low pressure, HKUST-1 exhibits a high adsorption capacity, showing the typical micro-porous nature of HKUST-1 with a *t*-plot micropore volume of 0.24 $m^3 g^{-1}$. The Brunauer–Emmett–Teller (BET) surface area of the as-synthesized HKUST-1 was 645 $m^2 g^{-1}$, which is close to the reported value by Münch and Mertens [50] under similar conditions. It must be noted that the value of the surface area is relatively low compared to other MOF structures but this value is related to the mild reaction conditions (i.e., ambient pressure, mild temperature, no microwave) used as well as the short duration of the reaction (1 h compared to days in some reported syntheses).

3.2. Oil droplets removal by HKUST-1: kinetic analysis

Using HKUST-1 to remove oil droplets from water is demonstrated by a set of sequential pictures in Fig. 2 to provide a qualitative evaluation of HKUST-1's capability. The 20-ml vial filled with a milky solution in Fig. 2(a) was the O/W emulsion and its oil concentration was 300 mg L^{-1}. Because of the light-scattering nature of the emulsion, the opacity of the vial masks the logo on the background. Once HKUST-1 was added to the O/W emulsion and dispersed in the emulsion, the resulting mixture exhibited a light-blue color as shown in Fig. 2(b). This is due to the blue color of HKUST-1. After 50-min shaking on the orbital shaker at ambient temperature, the vial was placed on a bench and the solution and HKUST-1 powders started to separate. Since the density of HKUST-1 (~1.22 g cm^{-1}) [60] is higher than water, HKUST-1 settled down to the bottom of the vial to complete the phase separation. In Fig. 2(c), the vial can be clearly seen through and the logo behind the vial is clearly visible. This result evidently proved that at least the bulk of the oil droplets were removed in the presence of HKUST-1.

We also recovered the used HKUST-1 from the solution and analyzed the sample using FT-IR spectroscopy. The spectrum of the used HKUST-1 is shown in Fig. 1(a) as the "oil-rich HKUST-1". The oil-rich HKUST displays similar bands as the pristine HKUST-1 while two singlet bands at 2854 and 2926 cm^{-1} are observed on the spectrum of the oil-rich HKUST-1. The bands at 2854 and 2926 cm^{-1} are characteristics of soybean oil and correspond to the C—H stretching mode of saturated C—C bonds [58]. The appearance of these bands on the spectrum of oil-rich HKUST-1 indicates that oil droplets were captured and "trapped" by HKUST-1.

Additionally, we observed that the powder of bulk HKUST-1 was fine and well-dispersed in the emulsion in the beginning of the reaction but aggregated as clusters in the end of the test. These clusters might form due to accumulation of oil droplets on the HKUST-1's surface. The accumulation of oil wrapped HKUST-1 so that the oil-rich HKUST-1 tended to coalesce to form the clusters, suggesting that HKUST-1 can act as a coagulant to facilitate coalescence of oil droplets in water. The aggregation of HKUST-1 may facilitate the settlement of HKUST-1 and accelerate the separation of HKUST-1 from water.

In order to quantitatively evaluate the capacity of HKUST-1 for the removal of oil droplets and investigate the removal mechanism, we conducted experiments of oil removal kinetics and equilibrium isotherms. In each experiment, an O/W emulsion with a concentration C_0 (mg L^{-1}) and a volume V (ml) was prepared. A dose of dry HKUST-1 powder m (g) then was added into the emulsion and placed on the orbital shaker for a period of reaction (mixing) time t. The residual concentration of the emulsion C_t (mg L^{-1}) was determined and the removal capacity q_t of oil droplets by HKUST-1 was calculated as follows:

$$q_t = \frac{V(C_0 - C_t)}{m} \quad (1)$$

At first, we investigated the effect of the reaction time on the removal capacity of HKUST-1. Fig. 3(a) displays the removal capacity by HKUST-1 as a function of the reaction time ranging from 0 to

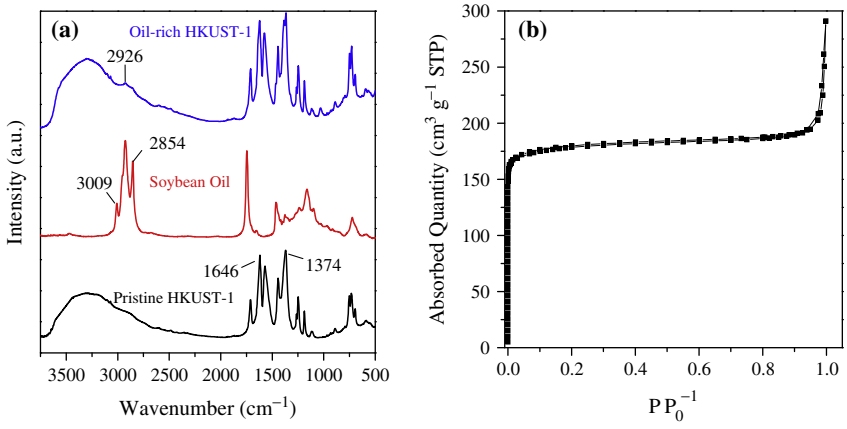

Fig. 1. Chemical and physical properties of HKUST-1: (a) IR spectra of pristine HKUST-1, soybean oil, and the oil-rich HKUST-1. (b) Nitrogen adsorption–desorption isotherm of HKUST-1 at 77 K.

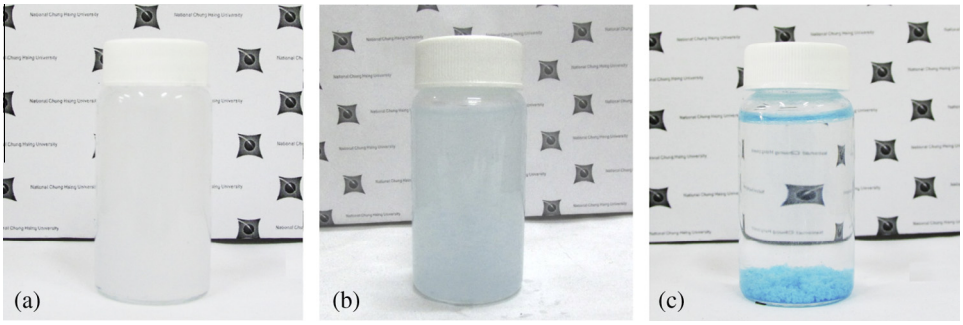

Fig. 2. Sequential pictures to show the oil droplets removed by HKUST-MOF from water. (a) O/W emulsion. Milky color of the emulsion blocks the NCHU logo on the background. (b) A mixture of HKUST-1 and the emulsion. The suspension becomes light-blue, indicating that HKUST-1 is evenly dispersed in the emulsion. (c) Oil droplet removed by HKUST-1 from water. The vial becomes transparent and the NCHU logo can be seen through the vial; oil droplets are successfully removed by HKUST-1. (For interpretation of the references to colour in this figure legend, the reader is referred to the web version of this article.)

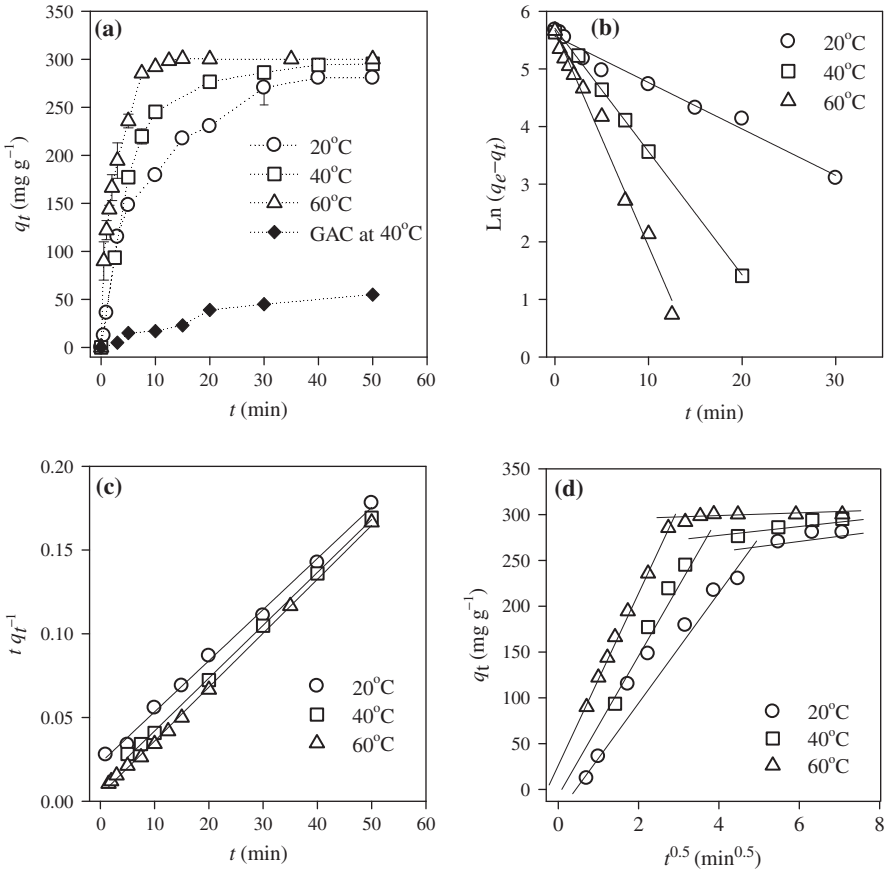

Fig. 3. Kinetics of the removal of oil droplets by HKUST-1: (a) removal capacity as a function of reaction time, (b) analysis of kinetic data using the pseudo first order equation, (c) analysis of kinetic data using the pseudo second order equation and (d) analysis of kinetic data using the intraparticle diffusion.

120 min at three different temperatures including 20, 40 and 60 °C. Each experiment was performed with an emulsion volume of 30 ml, an initial oil concentration of 300 mg L^{-1}, and a HKUST-1 dose of 0.02 g. The results in Fig. 3(a) reveal that at the beginning of the reaction, HKUST-1 possesses relatively high capacity, yet loses its capacity as the removal equilibrium is reached. We also investigated the effect of temperature on the time required to reach the equilibrium. At 20 °C, the removal capacity of HKUST-1 reaches its equilibrium after 50 min; at 40 °C and 60 °C, the equilibrium for the removal capacity of HKUST-1 can be reached in 40 min and 15 min, respectively. The effect of the temperature remarkably reduces the equilibrium time of the oil removal. The equilibrium removal capacities of HKUST-1 at the three temperatures were all close to 300 mg g^{-1} (as listed in Table 1, $q_{e,exp}$), showing that the oil droplets were removed from water.

The performance of HKUST-1 to separate oil/water mixture was compared to that of a granular activated carbon (GAC) at 40 °C [61]. As shown in Fig. 3(a), after 50 min of mixing, the removal capacity of GAC just reached 50 mg g^{-1}. This corresponds to only one sixth of the equilibrium removal capacity of HKUST-1. Evidently, the capacity of HKUST-1 to remove oil droplets was high. To further study the effect of temperature on the reaction

Table 1
Kinetic data of oil droplets removal by HKUST-1 at different conditions derived from the pseudo-first-order equation, the pseudo-second-order equation and the intraparticle diffusion model.

Condition	$q_{e,exp}$ (mg g^{-1})	Pseudo-first-order			Pseudo-second-order				The intraparticle diffusion	
		k_1 (min^{-1})	$q_{e,fitted}$ (mg g^{-1})	R_1^2	$k_2 \times 10^3$ (g mg^{-1} min^{-1})	$q_{e,fitted}$ (mg g^{-1})	h (mg g^{-1} min^{-1})	R_2^2	k_P (g mg^{-1} min$^{-0.5}$)	$R_P{}^2$
20 °C	295.29	0.081	262.13	0.978	0.42	322.58	43.80	0.996	57.64	0.947
40 °C	280.66	0.214	300.09	0.999	0.98	312.50	96.19	0.999	88.02	0.990
60 °C	300.20	0.375	290.32	0.987	2.69	312.50	263.08	0.998	94.54	0.998
NaCl, 40 °C	288.17	0.279	166.75	0.939	2.42	303.03	454.15	0.998	81.80	0.957
CTAB, 40 °C	292.55	0.376	203.56	0.978	5.25	294.11	222.22	0.998	110.34	0.971
pH = 4, 40 °C	281.12	0.279	166.71	0.939	4.95	303.03	454.54	0.999	113.87	0.939
pH = 10, 40 °C	288.00	0.285	177.64	0.992	3.88	303.03	357.14	0.999	76.69	0.967

kinetics quantitatively, q_t and t are analyzed using the pseudo first order equation, the pseudo second equation and the intraparticle diffusion. The pseudo first order equation can be expressed as follows:

$$\log(q_e - q_t) = \log q_e - \frac{k_1}{2.303} t \quad (2)$$

where q_t and q_e are the removal capacity (mg g^{-1}) at the reaction time t (min) and at equilibrium, respectively, and k_1 (min^{-1}) is the rate constant for the pseudo first order equation. The results of regression fitting using the pseudo first order equation at the three different temperatures are shown in Fig. 3(b). The kinetic constant k_1, the fitted equilibrium removal capacity $q_{e,fitted}$, the coefficient of determination R_1^2 are listed in Table 1, which reveals that a higher reaction temperature leads to a higher kinetic constant: a faster reaction rate towards the equilibrium. The estimated equilibrium removal capacities using the pseudo first order equation are all close to the experimental values and R_1^2 of the regression fitting are all higher than 0.97.

On the other hand, the modeling of kinetic data using the pseudo second order equation employed the following equation:

$$\frac{t}{q_t} = \frac{1}{k_2 q_e^2} + \frac{1}{q_e} t \quad (3)$$

where k_2 (g mg^{-1} min^{-1}) represents the rate constant for the pseudo second order equation.

Fig. 3(c) shows the regression fitting of the kinetic data using the pseudo second order equation. The kinetic constant k_2, the fitted equilibrium removal capacity $q_{e,fitted}$, the coefficient of determination R_2^2 are also listed in Table 1. The reaction at a higher temperature also leads to a higher k_2; the $q_{e,fitted}$ estimated by the pseudo second order equation are higher than the experimental removal capacities $q_{e,exp}$. However R_2^2 are all higher than 0.995, indicating that the pseudo second order equation is a more satisfactory model than the pseudo first order equation for the interpretation of the kinetic data of oil removal by HKUST-1.

Since HKUST-1 is a porous material, we also investigated the transfer of oil droplets from the external surface of HKUST-1 to the surface inside the pores of HKUST-1 using the intraparticle diffusion model as follows:

$$q_t = k_P t^{0.5} + C \quad (4)$$

where k_P represents the diffusion rate constant and C is the intercept. Generally the adsorption process progresses in three consecutive stages: the first stage of the external surface adsorption or the instantaneous adsorption, the second stage of the gradual adsorption, and the third stage of the final equilibrium of the adsorption [62,63]. In the second stage of the gradual adsorption, the intraparticle diffusion is a rate-limiting step and in the third stage, the intraparticle diffusion process slows down due to the low residual concentration of solutes [64].

According to Eq. (4), the q_t as a function of $t^{0.5}$ at the different temperatures was plotted in Fig. 3(d) in which the curves of q_t versus $t^{0.5}$ essentially consist of two linear components. The first sharp linear component represents the boundary layer diffusion and the second linear component is attributed to the intra-particle or pore diffusion. Table 1 also lists the boundary layer diffusion rate constants of the first linear component with their corresponding coefficients of determination. As the temperature rose from 20 to 60 °C, the boundary layer diffusion rate constant increased from 57.64 to 94.54 g mg^{-1} min$^{-0.5}$, indicating a higher reaction temperature facilitates the diffusion especially in the beginning of the adsorption process.

3.3. Sorption equilibrium of oil droplets on HKUST-1

Using HKUST-1 to remove oil droplets involves a dynamic equilibrium of oil concentration between two phases: water and HKUST-1. The equilibrium is essentially important to evaluate the feasibility of practical operations and to design an optimal process. Thus, it is necessary to establish a correlation between the equilibrium removal capacities and the residual concentrations. Consequently, we conducted a series of experiments with various initial concentrations of oil C_0 from 480 to1100 mg L^{-1}, and a fixed amount of HKUST-1 (m = 0.02 g). The adsorption experiments were performed for at least 90 min to ensure that the reaction reached the equilibrium. To analyze the equilibrium data, two common adsorption isotherms, the Langmuir adsorption isotherm and the Freundlich adsorption isotherm, were employed. The Langmuir adsorption isotherm has been used in many cases of adsorption of a solute from a solution and the isotherm model assumes that the adsorption occurs on the specific homogenous sites on the surface of the adsorbent. The Langmuir adsorption isotherm is recognized as one of the most employed methods to quantify and compare the performance of various adsorbents with predication of maximal solute uptake. The fully-occupied monolayer isotherm can be described as follows:

$$q_e = \frac{q_{max} K_L C_e}{1 + K C_e} \quad (5)$$

where q_{max} and K_L are the Langmuir model constants, representing adsorption capacity and bonding energy constant, respectively, and C_e is the remaining oil concentration at the equilibrium.

The Freundlich isotherm, on the other hand, represents an empirical expression that includes the heterogeneity of the surface and an exponential distribution of the sites and their energies. This isotherm has been further extended by considering the influence of adsorption sites and the competition between different adsorbents for adsorption on available sites. The Freundlich isotherm has been observed to be applicable for a wide range of heterogeneous surfaces including activated carbon, silica, clays, and polymers. The Freundlich isotherm can be described as follows:

$$q_e = K_F C_e^{1/n} \quad (6)$$

where $1/n$ is the heterogeneity factor of the adsorbent, K_F is a constant and C_e is the remaining oil concentration at the equilibrium.

The surface heterogeneity is attributed to the existences of crystal edges, cations, surface charges, surface functional groups, and degrees of crystallinity of the surface. The $1/n$ value determines the relative distribution of energy sites and depends on the nature and strength of the adsorption process.

The equilibrium data at 40 °C of oil droplet removal by HKUST-1 is shown in Fig. 4(a), in which the equilibrium removal capacity q_e increases as the initial concentration of oil C_0 becomes higher yet reaches a maximal q_e as C_0 exceeds a certain value. The insets (Fig. 4(b) and (c)) are the regression fitting curves of the experimental equilibrium data using the Langmuir isotherm model and the Freundlich isotherm model, respectively. According to Eqs. (5) and (6), the corresponding model constants, including the coefficients of determination (R^2), were calculated and the results are listed in Table 2.

The maximal equilibrium removal capacity q_{max} of HKUST-1 is 4000 mg g^{-1} and the Langmuir equilibrium constant K_L is 0.184 L mg^{-1} with $R_L{}^2$ of 0.997. The high q_{max} indicates the promising capability of HKUST-1 to remove oil droplets from water. The factors leading such a high removal capacity may be attributed to the existence of benzene rings from H_3BTC and the unsaturated metal centers of HKUST-1 [40,65]. The benzene rings in HKUST-1 have been suggested to attract hydrophobic compounds which are typically encountered in the soybean oil used in the present study [42]. Besides, the unsaturated copper centers of HKUST-1 can act as Lewis acids [66,67]. The metal sites may therefore attract electron-rich unsaturated fatty acids in the soybean oil.

On the other hand, the Freundlich equilibrium constant is 3.176 (mg g^{-1}) (L mg^{-1})$^{1/n}$, the amount removed at unit concentration is 1 mg L^{-1} and the empirical constant n is 0.213 with $R_F{}^2$ of 0.889. Since the value of $R_L{}^2$ is noticeably higher than $R_F{}^2$ and the value approximates to 1, the Langmuir model appears as a more satisfactory to interpret the equilibrium data.

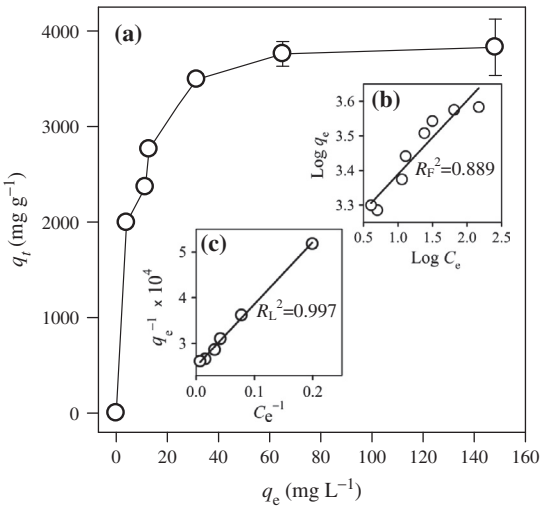

Fig. 4. Equilibrium data and analysis of the separation of oil droplet from water using HKUST-1: (a) adsorption isotherm of HKUST-1, (b) modeling of equilibrium data using Langmuir isotherm and (c) modeling of equilibrium data using Freundlich isotherm.

3.4. Effects of sodium chloride (NaCl) and cetrimonium bromide (CTAB)

To evaluate the effects of other compounds present in wastewater on the removal capacity of HKUST-1, we particularly investigated the variation of removal capacity of oil droplets by HKUST-1 in the presence of sodium chloride (NaCl) and cetrimonium bromide (CTAB). The addition of NaCl was used to study the effect of salts in water on the removal capacity and the addition of CTAB, a common surfactant and an organic salt, was used to examine the effect of surfactants in wastewater on the removal capacity. Experiments involving NaCl were performed by dissolving NaCl in D.I. water to obtain concentrated salty water and then adding it to the O/W emulsion prepared as described in Section 2. The final concentration of NaCl in the emulsion was set at 500 mg L^{-1} and the experiment was conducted at 40 °C. The removal capacities q_t versus t with and without the addition of NaCl are plotted in Fig. 5(a) and the analyses of the kinetic data using the pseudo first order, the second order and the intraparticle diffusion are also plotted (Fig. S2, ESI†) to obtain their corresponding rate constants. The derived constants are listed in Table 1. Although k_P in the presence of NaCl is comparable to k_P in the absence of NaCl, k_1 and k_2 in the presence of NaCl are both higher than those in the absence of NaCl. Therefore, NaCl significantly affected the sorption kinetics of oil droplets by HKUST-1: the sorption reached its equilibrium faster with the addition of NaCl.

On the other hand, the emulsion containing 500 mg L^{-1}of CTAB was also prepared and the removal capacity of HKUST-1 in the presence of CTAB was tested. The removal capacity q_t versus t in the presence of CTAB was plotted in Fig. 5(a) and the kinetic data was also analyzed using the pseudo first order equation, the second pseudo order equation and the intraparticle diffusion (Fig. S2, ESI†) to obtain their corresponding rate constants. The derived constants are listed in Table 1. The q_t in the presence of CTAB reaches its equilibrium faster than the q_t in the absence of CTAB. The rate constants of the pseudo first order, the pseudo second order and the boundary layer diffusion are all much higher than the rate constants of the three models for the "pure" oil/water system. This indicates the faster reaction rate in the oil removal in the presence of CTAB.

Both additions of NaCl and CTAB increased the oil-removal kinetics of HKUST-1; the faster kinetics could be due to a higher coalescence rate of oil droplets which might be induced by the change of surface charges of HKUST-1 in the presence of salts [68].

3.5. Effect of the pH of oil emulsions

The pH of the emulsion considerably affects the stability of oil droplets. To understand the effect of pH value on the removal efficiency of oil droplets by HKUST-1, we tested two emulsions with pH values adjusted to 4 and 10, representing a weakly acid condition and a weakly basic condition, respectively. The pH was controlled by addition of 0.1 M hydrochloric acid or 0.1 M sodium hydroxide solution. The pH of an unadjusted O/W emulsion was found to be 7, similar to the pH value of D.I. water because of the relatively low concentration (i.e., less than 1000 ppm) of oil. The effect of pH on the removal capacity was examined by comparing the removal capacities of HKUST-1 in a pH-unadjusted emul-

Table 2
Isotherm model constants derived from the Langmuir model and the Freundlich model.

Temperature	Langmuir			Freundlich		
	q_{max} (mg g^{-1})	K_L (L mg^{-1})	$R_L{}^2$	K_F (mg g^{-1}) (L mg^{-1})$^{1/n}$	n	$R_F{}^2$
40 °C	4000	0.184	0.997	23.950	4.700	0.899

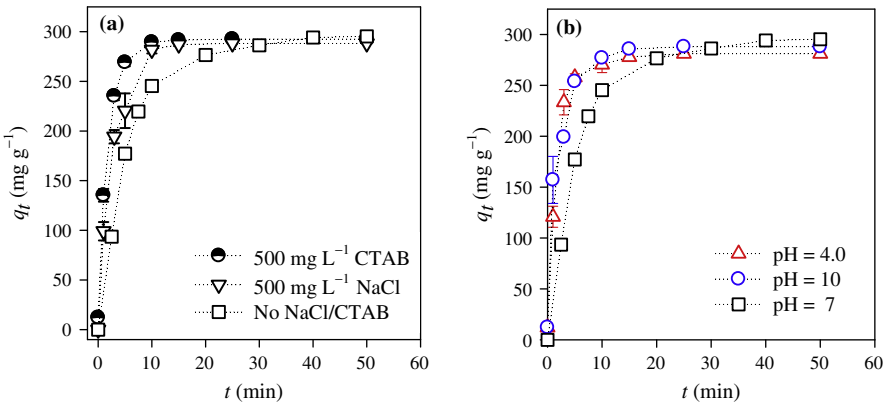

Fig. 5. Effects on the removal capacity of HKUST-1 of: (a) the addition of NaCl and CTAB and (b) the pH of the emulsion. HKUST-1 exhibits fast reaction rates in the emulsions containing the surfactant CTAB and the salt NaCl, and in the pH-adjusted emulsions.

sion with pH-adjusted emulsions. The removal kinetics of the weakly acidic, neutral, and weakly basic emulsions by HKUST-1 is shown in Fig. 5(b). The rate constants of the pseudo first order, the pseudo second order and the boundary layer diffusion also obtained using the three models (Fig. S3, ESI†). The kinetic constants were also listed in Table 1. For the weakly acidic emulsion the neutral emulsion, the weakly basic emulsion, their k_1 are 0.279, 0.214 and 0.285 min^{-1}, respectively. As a result, HKUST-1 in the pH-adjusted emulsion exhibited faster removal kinetics than in the pH-unadjusted emulsion. A similar result was obtained by comparing k_2 in the pH-adjusted and pH-unadjusted emulsions. While k_P in the weakly basic emulsion is comparable to the k_P in the neutral emulsion, k_P in the weakly acidic emulsion is noticeably higher.

Faster oil-removal kinetics of HKUST-1 in the weakly acidic and weakly basic emulsions may be attributed to a higher coalescence rate in the emulsions. Since oil droplets are generally stabilized by the repulsive surface charges, additions of acids and bases can change the interfacial properties and therefore disturb the stability of the emulsion and increase the coalescence rate [69–71].

3.6. Recyclability test of HKUST for removal of oil droplets

The recyclability of HKUST-1 for oil removal is as important as its capacity. Considering the rapidity and efficiency required for oil removal applications, HKUST-1 must be regenerated by a simple and convenient method. In this study, we tested the regeneration by washing the oil-rich HKUST-1 with ethanol. Oil droplets are readily soluble in ethanol because ethanol is a less-polar solvent compared with water. The removal capacity of the regenerated HKUST-1 is shown in Fig. 6(a). The first cycle of regeneration allowed HKUST-1 to exhibit almost identical removal capacity as the pristine HKUST-1. The subsequent regeneration cycles also enabled HKUST-1 to exhibit the similar removal capacity, showing that the ethanol-washing process represents an efficient and convenient method to recycle HKUST-1 after oil removal. Additionally, to examine the effect of regeneration on the structural properties of HKUST-1, we also conducted N_2 sorption and desorption experiments on the regenerated HKUST-1. The surface area and pore volume of HKUST-1 after regeneration were found to decrease by 8% and 15%, respectively. These changes did not reflect on the removal capacity of HKUST-1 for oil, suggesting that the main mechanism of removing oil droplets by HKUST-1 mainly involved the specific functional groups with HKUST-1 (e.g., benzene rings) as discussed in the earlier section.

3.7. Thermogravimetric analysis of oil-adsorbed HKUST-1

In addition to the ethanol-washing process, elevated temperatures may be an alternative method to remove oil from the oil-rich HKUST-1. Fig. 6(b) shows the derivative thermogravimetric (DTG) analyses of pristine HKUST-1 and the oil-rich HKUST-1. For the pristine HKUST-1, weight loss firstly occurs at around 100 °C due to water evaporation and then at 275 °C because of the decomposition of HKUST-1 [60]. For the oil-rich HKUST-1, the DTG curve is similar to that of the pristine HKUST-1. However the oil-rich HKUST-1 displays an additional weight loss at 177 °C which is the smoke point of common semi-refined soybean oil [72,73]. This

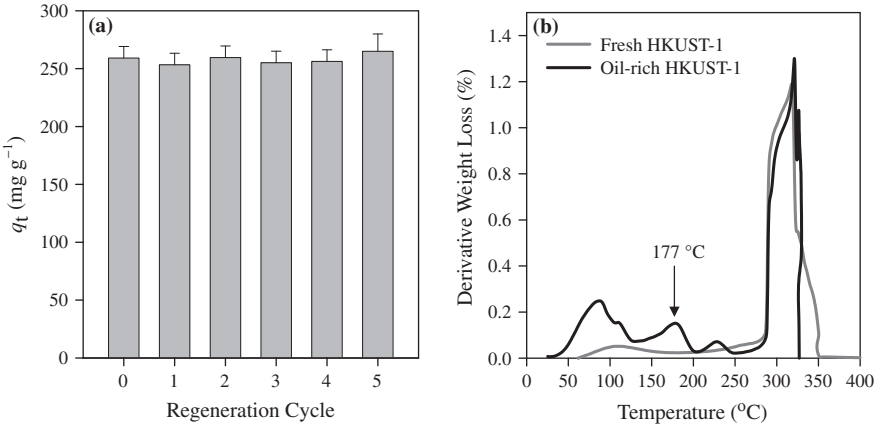

Fig. 6. Recyclability of HKUST-1: (a) removal capacities of a five-cycle test, (b) DTG curves of HKUST-1 and the oil-rich HKUST-1 in N_2. The oil-rich HKUST-1 was generated by washing with ethanol for 30 min. Before the thermal decomposition of HKUST-1, the oil is burnt and released from HKUST-1 at 177 °C.

result suggests that the oil can be removed from the oil-rich HKUST-1 at elevated temperatures that are lower than the thermal decomposition temperature of HKUST-1.

4. Conclusion

In this study, we have successfully demonstrated the use of HKUST-1 to remove oil droplets from water. HKUST-1 can be well-dispersed in the O/W emulsion and capture oil droplets after a certain time of mixing. Once oil droplets are adsorbed on HKUST-1, the oil-rich HKUST-1 tends to coagulate and settles down in the aqueous phase to complete the phase change. The kinetic data analysis indicates that the removal of oil droplets can be modeled by the pseudo second order equation. On the other hand, adsorption equilibrium data are well represented by the Langmuir isotherm model.

A higher reaction temperature was found to increase the reaction rate constants, suggesting that the reaction of oil droplets removed by HKUST-1 may be endothermic. HKUST-1 exhibited 6 times the oil-removal capacity of activated carbon under the same condition. The maximal removal capacity of HKUST-1 estimated by the Langmuir isotherm model was 4000 mg g^{-1}. Additions of NaCl and CTAB to the emulsions, as well as change of the pH of the emulsions increased the reaction rate of oil removal likely due to the faster coalescence rate of oil droplets. HKUST-1 was successfully regenerated using an ethanol washing process. The sample exhibited at least 95% of its original removal capacity during the 5 testing cycles.

The high capacity of HKUST-1 and good recyclability for oil removal evidences the promising potential of HKUST-1 for applications in which hydrophobic phase must be separated from a hydrophilic phase. Examples include wastewater treatment plants, food processing and biological areas. Further studies should be continued on the removal of different oils from hydrophilic phases.

Acknowledgement

We appreciate the Center of Nanoscience & Nanotechnology at National Chung Hsing University for the assistance on electronic microscopic analysis. We are also grateful for the funding support from the Ministry of Science and Technology on the project NSC 102-2218-E-005-003.

Appendix A. Supplementary material

Supplementary data associated with this article can be found, in the online version, at http://dx.doi.org/10.1016/j.cej.2014.03.107.

References

[1] R.F. Johnson, T.G. Manjreker, J.E. Halligan, Removal of oil from water surfaces by sorption on unstructured fibers, Environ. Sci. Technol. 7 (1973) 439–443.
[2] K.K. Salam, A.O. Alade, A.O. Arinkoola, A. Opawale, Improving the demulsification process of heavy crude oil emulsion through blending with diluent, J. Petrol. Eng. 2013 (2013) 6.
[3] H. Wang, K.-Y. Lin, B. Jing, G. Krylova, G.E. Sigmon, P. McGinn, Y. Zhu, C. Na, Removal of oil droplets from contaminated water using magnetic carbon nanotubes, Water Res. 47 (2013) 4198–4205.
[4] A. Takamura, F. Ishii, S.I. Noro, M. Koishi, Physicopharmaceutical characteristics of an oil-in-water emulsion-type ointment containing diclofenac sodium, J. Pharm. Sci. 73 (1984) 676–681.
[5] E.N. Frankel, S.-W. Huang, R. Aeschbach, E. Prior, Antioxidant activity of a rosemary extract and its constituents, carnosic acid, carnosol, and rosmarinic acid, in bulk oil and oil-in-water emulsion, J. Agric. Food Chem. 44 (1996) 131–135.
[6] D. Djordjevic, D.J. McClements, E.A. Decker, Oxidative stability of whey protein-stabilized oil-in-water emulsions at pH 3: potential ω-3 fatty acid delivery systems (Part B), J. Food Sci. 69 (2004) C356–C362.
[7] U. Klinkesorn, P. Sophanodora, P. Chinachoti, D.J. McClements, Stability and rheology of corn oil-in-water emulsions containing maltodextrin, Food Res. Int. 37 (2004) 851–859.
[8] J.W. Paterson, Industrial Wastewater Treatment Technology, Butterworth Publishers, 1985.
[9] M. Quéméneur, Y. Marty, Fatty acids and sterols in domestic wastewaters, Water Res. 28 (1994) 1217–1226.
[10] D. Wang, T. Silbaugh, R. Pfeffer, Y.S. Lin, Removal of emulsified oil from water by inverse fluidization of hydrophobic aerogels, Powder Technol. 203 (2010) 298–309.
[11] Y.-B. Zhou, X.-Y. Tang, X.-M. Hu, S. Fritschi, J. Lu, Emulsified oily wastewater treatment using a hybrid-modified resin and activated carbon system, Sep. Purif. Technol. 63 (2008) 400–406.
[12] S. Ibrahim, S. Wang, H.M. Ang, Removal of emulsified oil from oily wastewater using agricultural waste barley straw, Biochem. Eng. J. 49 (2010) 78–83.
[13] H. Maruyama, H. Seki, Y. Satoh, Removal kinetic model of oil droplet from o/w emulsion by adding methylated milk casein in flotation, Water Res. 46 (2012) 3094–3100.
[14] N. Hilal, G. Busca, N. Hankins, A.W. Mohammad, The use of ultrafiltration and nanofiltration membranes in the treatment of metal-working fluids, Desalination 167 (2004) 227–238.
[15] A. Lobo, Á. Cambiella, J.M. Benito, C. Pazos, J. Coca, Ultrafiltration of oil-in-water emulsions with ceramic membranes: influence of pH and crossflow velocity, J. Membr. Sci. 278 (2006) 328–334.
[16] B. Hu, K. Scott, Influence of membrane material and corrugation and process conditions on emulsion microfiltration, J. Membr. Sci. 294 (2007) 30–39.
[17] G. Ríos, C. Pazos, J. Coca, Destabilization of cutting oil emulsions using inorganic salts as coagulants, Colloid Surf. A Physicochem. Eng. Aspects 138 (1998) 383–389.
[18] P. Cañizares, F. Martínez, C. Jiménez, C. Sáez, M.A. Rodrigo, Coagulation and electrocoagulation of oil-in-water emulsions, J. Hazard. Mater. 151 (2008) 44–51.
[19] M. Carmona, M. Khemis, J.-P. Leclerc, F. Lapicque, A simple model to predict the removal of oil suspensions from water using the electrocoagulation technique, Chem. Eng. Sci. 61 (2006) 1237–1246.
[20] S.I. Abo-El Ela, S.S. Nawar, Treatment of wastewater from an oil and soap factory via dissolved air flotation, Environ. Int. 4 (1980) 47–52.
[21] A.I. Zouboulis, A. Avranas, Treatment of oil-in-water emulsions by coagulation and dissolved-air flotation, Colloids Surf. A 172 (2000) 153–161.
[22] A.A. Al-Shamrani, A. James, H. Xiao, Separation of oil from water by dissolved air flotation, Colloids Surf. A 209 (2002) 15–26.
[23] A.A. Al-Shamrani, A. James, H. Xiao, Destabilisation of oil–water emulsions and separation by dissolved air flotation, Water Res. 36 (2002) 1503–1512.
[24] M.N. Rashed, Adsorption Technique for the Removal of Organic Pollutants from Water and Wastewater, 2013.
[25] H. Moazed, T. Viraraghavan, Use of organo-clay/anthracite mixture in the separation of oil from oily waters, Energy Sources 27 (2005) 101–112.
[26] V. Rajakovic, G. Aleksic, M. Radetic, L. Rajakovic, Efficiency of oil removal from real wastewater with different sorbent materials, J. Hazard. Mater. 143 (2007) 494–499.
[27] G. Alther, Cleaning wastewater: removing oil from water with organoclays, Filtr. Sep. 45 (2008) 22–24.
[28] H. Moazed, T. Viraraghavan, Removal of oil from water by bentonite organoclay, Pract. Periodical Hazard. Toxic Radioactive Waste Manage. 9 (2005) 130–134.
[29] N. Stock, S. Biswas, Synthesis of Metal–Organic Frameworks (MOFs): routes to various MOF topologies, Morphol. Compos. Chem. Rev. 112 (2011) 933–969.
[30] C. Janiak, J.K. Vieth, MOFs, MILs and more: concepts, properties and applications for porous coordination networks (PCNs), New J. Chem. 34 (2010) 2366–2388.
[31] U. Mueller, M. Schubert, F. Teich, H. Puetter, K. Schierle-Arndt, J. Pastre, Metal–organic frameworks–prospective industrial applications, J. Mater. Chem. 16 (2006) 626–636.
[32] J.W. Yoon, S.H. Jhung, Y.K. Hwang, S.M. Humphrey, P.T. Wood, J.S. Chang, Gas-sorption selectivity of CUK-1: a porous coordination solid made of cobalt(II) and pyridine-2,4- dicarboxylic acid, Adv. Mater. 19 (2007) 1830–1834.
[33] J.-R. Li, Y. Ma, M.C. McCarthy, J. Sculley, J. Yu, H.-K. Jeong, P.B. Balbuena, H.-C. Zhou, Carbon dioxide capture-related gas adsorption and separation in metal–organic frameworks, Coord. Chem. Rev. 255 (2011) 1791–1823.
[34] J.-R. Li, R.J. Kuppler, H.-C. Zhou, Selective gas adsorption and separation in metal–organic frameworks, Chem. Soc. Rev. 38 (2009) 1477–1504.
[35] J. Lee, O.K. Farha, J. Roberts, K.A. Scheidt, S.T. Nguyen, J.T. Hupp, Metal–organic framework materials as catalysts, Chem. Soc. Rev. 38 (2009) 1450–1459.
[36] A. Corma, H. García, F.X. Llabrés i Xamena, Engineering metal organic frameworks for heterogeneous catalysis, Chem. Rev. 110 (2010) 4606–4655.
[37] J. Gascon, A. Corma, F. Kapteijn, F.X. Llabrés i Xamena, Metal organic framework catalysis: quo vadis?, ACS Catal (2013) 361–378.
[38] P. Horcajada, T. Chalati, C. Serre, B. Gillet, C. Sebrie, T. Baati, J.F. Eubank, D. Heurtaux, P. Clayette, C. Kreuz, J.-S. Chang, Y.K. Hwang, V. Marsaud, P.-N. Bories, L. Cynober, S. Gil, G. Ferey, P. Couvreur, R. Gref, Porous metal-organic-framework nanoscale carriers as a potential platform for drug delivery and imaging, Nat. Mater. 9 (2010) 172–178.
[39] L.-G. Qiu, Z.-Q. Li, Y. Wu, W. Wang, T. Xu, X. Jiang, Facile synthesis of nanocrystals of a microporous metal–organic framework by an ultrasonic method and selective sensing of organoamines, Chem. Commun. (2008) 3642–3644.

[40] F. Ke, L.-G. Qiu, Y.-P. Yuan, F.-M. Peng, X. Jiang, A.-J. Xie, Y.-H. Shen, J.-F. Zhu, Thiol-functionalization of metal–organic framework by a facile coordination-based postsynthetic strategy and enhanced removal of Hg^{2+} from water, J. Hazard. Mater. 196 (2011) 36–43.
[41] L. Li, J.C. Li, Z. Rao, G.W. Song, B. Hu, Metal organic framework $[Cu_3(BTC)_2(H_2O)_3]$ for the adsorption of methylene blue from aqueous solution, Desalination Water Treat. (2013) 1–7.
[42] B.K. Jung, Z. Hasan, S.H. Jhung, Adsorptive removal of 2,4-dichlorophenoxyacetic acid (2,4-D) from water with a metal–organic framework, Chem. Eng. J. 234 (2013) 99–105.
[43] A. Banerjee, R. Gokhale, S. Bhatnagar, J. Jog, M. Bhardwaj, B. Lefez, B. Hannoyer, S. Ogale, MOF derived porous carbon–Fe_3O_4 nanocomposite as a high performance, recyclable environmental superadsorbent, J. Mater. Chem. 22 (2012) 19694–19699.
[44] C. Yang, U. Kaipa, Q.Z. Mather, X. Wang, V. Nesterov, A.F. Venero, M.A. Omary, Fluorous metal–organic frameworks with superior adsorption and hydrophobic properties toward oil spill cleanup and hydrocarbon storage, J. Am. Chem. Soc. 133 (2011) 18094–18097.
[45] J. Kim, H.-Y. Cho, W.-S. Ahn, Synthesis and adsorption/catalytic properties of the metal organic framework CuBTC, Catal. Surv. Asia 16 (2012) 106–119.
[46] A. Dhakshinamoorthy, M. Opanasenko, J. Čejka, H. Garcia, Metal organic frameworks as solid catalysts in condensation reactions of carbonyl groups, Adv. Synth. Catal. 355 (2013) 247–268.
[47] E. Perez-Mayoral, Z. Musilova, B. Gil, B. Marszalek, M. Polozij, P. Nachtigall, J. Cejka, Synthesis of quinolines via Friedlander reaction catalyzed by CuBTC metal–organic-framework, Dalton Trans. 41 (2012) 4036–4044.
[48] M. Opanasenko, A. Dhakshinamoorthy, M. Shamzhy, P. Nachtigall, M. Horacek, H. Garcia, J. Cejka, Comparison of the catalytic activity of MOFs and zeolites in Knoevenagel condensation, Catal. Sci. Technol. 3 (2013) 500–507.
[49] M. Opanasenko, M. Shamzhy, J. Čejka, Solid acid catalysts for coumarin synthesis by the Pechmann reaction: MOFs versus zeolites, ChemCatChem 5 (2013) 1024–1031.
[50] A.S. Münch, F.O.R.L. Mertens, HKUST-1 as an open metal site gas chromatographic stationary phase-capillary preparation, separation of small hydrocarbons and electron donating compounds, determination of thermodynamic data, J. Mater. Chem. 22 (2012) 10228–10234.
[51] A. Ahmed, M. Forster, R. Clowes, D. Bradshaw, P. Myers, H. Zhang, Silica SOS@HKUST-1 composite microspheres as easily packed stationary phases for fast separation, J. Mater. Chem. A 1 (2013) 3276–3286.
[52] D. Peralta, K. Barthelet, J. Pérez-Pellitero, C. Chizallet, G. Chaplais, A. Simon-Masseron, G.D. Pirngruber, Adsorption and separation of xylene isomers: CPO-27-Ni vs HKUST-1 vs NaY, J. Phys. Chem. C 116 (2012) 21844–21855.
[53] S. Ma, H.-C. Zhou, Gas storage in porous metal–organic frameworks for clean energy applications, Chem. Commun. 46 (2010) 44–53.
[54] A. Venkatasubramanian, J.-H. Lee, R.J. Houk, M.D. Allendorf, S. Nair, P.J. Hesketh, Characterization of HKUST-1 crystals and their application to mems microcantilever array sensors, ECS Trans. 33 (2010) 229–238.
[55] T.W. Patzek, A first law thermodynamic analysis of biodiesel production from soybean, Bull. Sci. Technol. Soc. 29 (2009) 194–204.
[56] L.D. O'Neill, H. Zhang, D. Bradshaw, Macro-/microporous MOF composite beads, J. Mater. Chem. 20 (2010) 5720–5726.
[57] L.H. Wee, M.R. Lohe, N. Janssens, S. Kaskel, J.A. Martens, Fine tuning of the metal–organic framework $Cu_3(BTC)_2$ HKUST-1 crystal size in the 100 nm to 5 μm range, J. Mater. Chem. 22 (2012) 13742–13746.
[58] N.A. Gomez, R. Abonia, H. Cadavid, I.H. Vargas, Chemical and spectroscopic characterization of a vegetable oil used as dielectric coolant in distribution transformers, J. Braz. Chem. Soc. 22 (2011) 2292–2303.
[59] L. Peng, J. Zhang, J. Li, B. Han, Z. Xue, B. Zhang, J. Shi, G. Yang, Hollow metal–organic framework polyhedra synthesized by a CO_2–ionic liquid interfacial templating route, J. Colloid Interface Sci. 416 (2014) 198–204.
[60] S.S.-Y. Chui, S.M.-F. Lo, J.P.H. Charmant, A.G. Orpen, I.D. Williams, A chemically functionalizable nanoporous material $[Cu_3(TMA)_2(H_2O)_3]_n$, Science 283 (1999) 1148–1150.
[61] M. Fulazzaky, R. Omar, Removal of oil and grease contamination from stream water using the granular activated carbon block filter, Clean Technol. Environ. Policy 14 (2012) 965–971.
[62] R. Han, P. Han, Z. Cai, Z. Zhao, M. Tang, Kinetics and isotherms of Neutral Red adsorption on peanut husk, J. Environ. Sci. 20 (2008) 1035–1041.
[63] X. Yu, G. Zhang, C. Xie, Y. Yu, T. Cheng, Q. Zhou, Equilibrium, kinetic, and thermodynamic studies of hazardous dye neutral red biosorption by spent corncob substrate, BioResources 6 (2011) 936–949.
[64] P. Luo, Y. Zhao, B. Zhang, J. Liu, Y. Yang, J. Liu, Study on the adsorption of Neutral Red from aqueous solution onto halloysite nanotubes, Water Res. 44 (2010) 1489–1497.
[65] P. Horcajada, C. Serre, A.C. McKinlay, R.E. Morris, Biomedical applications of metal–organic frameworks, in: Metal-Organic Frameworks, Wiley-VCH Verlag GmbH & Co. KGaA, 2011, pp. 213–250.
[66] L. Mitchell, B. Gonzalez-Santiago, J.P.S. Mowat, M.E. Gunn, P. Williamson, N. Acerbi, M.L. Clarke, P.A. Wright, Remarkable Lewis acid catalytic performance of the scandium trimesate metal organic framework MIL-100(Sc) for C–C and C[double bond, length as m-dash]N bond-forming reactions, Catal. Sci. Technol. 3 (2013) 606–617.
[67] H.-L. Jiang, Q. Xu, Nanoporous metal organic frameworks, Nanoporous Mater.: Synthe. Appl. (2013) 71–95.
[68] B.P. Binks, R. Murakami, S.P. Armes, S. Fujii, Effects of pH and salt concentration on oil-in-water emulsions stabilized solely by nanocomposite microgel particles, Langmuir 22 (2006) 2050–2057.
[69] C.-M. Chen, C.-H. Lu, C.-H. Chang, Y.-M. Yang, J.-R. Maa, Influence of pH on the stability of oil-in-water emulsions stabilized by a splittable surfactant, Colloids Surf. A 170 (2000) 173–179.
[70] K. Demetriades, J.N. Coupland, D.J. McClements, Physical properties of whey protein stabilized emulsions as related to pH and NaCl, J. Food Sci. 62 (1997) 342–347.
[71] J.E. Strassner, J. Petrol. Technol. 243 (1968) 303.
[72] C.V. Gauthier, G. Pinto, Spattering and crackle of hot cooking oil with water. A classroom demonstration and discussion, J. Chem. Educ. 86 (2009) 1281.
[73] M. Chu, Smoke Points of Various Fats, <http://www.cookingforengineers.com/article/50/SmokePointsofVariousFats> (accessed December 2013).